PAPER • OPEN ACCESS

Experimental study of air-water two-phase jet: bubble size distribution and velocity measurements

View the article online for updates and enhancements.

Experimental study of air-water two-phase jet: bubble size distribution and velocity measurements

Di Nunno Fabio[1], Alves Pereira Francisco[2], de Marinis Giovanni[1], Di Felice Fabio[2], Gargano Rudy[1], Granata Francesco[1], Miozzi Massimo[2]

[1]Department of Civil and Mechanical Engineering, University of Cassino and Southern Lazio, Cassino, FR, Italy
[2]CNR-INM (formerly INSEAN), Roma, Italy

fabio.dinunno@unicas.it

Abstract. An experimental investigation on a horizontal two-phase air-water jet has been conducted in order to develop a technique that can provide information on the interaction between the air bubbles and turbulent flow. In order to allow a measurement of the liquid phase flow field and of the bubbles size, the Particle Image Velocimetry (PIV) has been used, with the liquid phase seeded with a fluorescent tracer consisting of Rhodamine WT mixed with a commercial polyester resin. A phase discrimination algorithm has been developed and successfully used for the detection and separation of tracers and bubbles in distinct images. Three data sets have been recorded: one for a one-phase water jet and two for a two-phase water jet. The obtained results allow a valid characterization of the flow field and an estimation of the effect of the gaseous phase in the air-water jet flow. An analysis of the bubbles size and number has been also conducted and here reported.

1. Introduction

The study of two phase air-water flows is of great importance in many engineering applications, such as air entrainment mechanisms in sewer manhole [1] [2] and drag reduction by bubble injection in the boundary layers of the transport ships [3]. Most of the experimental studies conducted on these issues have as their objective the measurement of the flow field of the liquid phase and an evaluation of the air bubbles concentration. In order to have a complete characterization of the two-phase flow, both in terms of flow field of the two phases and of the concentration, distribution and geometry of the bubbles, the Particle Image Velocimetry (PIV) has been used for this study. However, PIV has been widely used in past for experimental activities on single-phase water flow or for two-phase air-water flows with a simple dynamic and a low void fraction [4]. In addition, an accurate detection and separation of the two phases is a very complex task. Phase discrimination algorithms typically used for the PIV applications are based on the size of the seeding particles and secondary phase or on the wavelength of the scattered light of these elements. The "masking technique" [5], consisting in the introduction of a "mask" able to separate the objects larger or smaller than a certain threshold value, is one of the most widely used techniques for the phase discrimination [6]. However, a size discrimination method can be used only in the presence of a clear difference in the size of the elements constituting the different phases. Furthermore, in an image recorded with the PIV technique, when the seeding particles are illuminated by the laser light, they scatter a light that involves an increase in terms of particles recorded dimension. Therefore, in presence of a second phase with a minimum dimension not sufficiently high to overcome the minimum recorded size of the seeding particles, is necessary to use more complex discrimination

algorithms. In this sense, a new algorithm has been introduced and presented in this work for the phases discrimination. The algorithm, in addition to considering the size and the wavelength of the scattered light, also takes into account some characteristic parameters of each phase.

2. Study Methodology

2.1. Experimental Setup

The experimental apparatus (Figure 1) consists of a horizontal jet, with an outlet diameter D equal to 21mm, which enters in a horizontal parallelepiped Plexiglas tank 45D long, 9D wide and 20D high. The axis of the jet outlet section is placed at 6.5D from the bottom of the tank, 7.5D from the free surface, the latter adjusted by means of a rectangular weir, and 4.5D from the side walls. A centrifugal pump with a maximum flow rate of 40l/min has been used in order to allow the circulation of water in a closed loop. An air compressor with a maximum working pressure of 10bar has been used to inject air along a copper pipe. The water flow rate is measured by an electromagnetic flow meter, while a digital flow meter has been used to measure the air flow rate. The mixing between water and air takes place upstream of the tank and inside a High-Density PolyEthylene (HDPE) pipe, with diameter equal to D, through a coaxial copper pipe with a diameter of 6mm. The test section for the measurements, located near the jet outlet section, extends from 0 to about 9D streamwise and from -3.5D to 4D spanwise.

The high-speed PIV system consists in a CCD camera PowerView Plus 11MP, produced by TSI, with a resolution of 4000x2672pixels. The camera objective is a 50mm focal length, mapping an area of 250x167mm2. The laser light is provided by a double-pulsed Nd-YAG laser with a wavelength of 532nm, a frequency of 15Hz and maximum energy of 50mJ. The laser sheet, thickness equal to 4mm, is directed, through a mirror system, in the middle plane of the tank section. Water is seeded with a tracer, mean diameter of 128 μm and a density of 1.19 g/cm3, made from an aqueous solution of Rhodamine WT at 20% concentration in volume mixed with a commercial polyester resin [7]. When the seeding particle are illuminated by the laser sheet, they scattered a light with a wavelength of 545-590nm, different from the laser light. In order to remove the reflections due to the non-Lambertian nature of the scatter on the surface of the bubbles from the recorded image, a high pass filter with a wavelength of 550nm is located on the camera objective. This allows to record images containing exclusively the tracers, related to the liquid phase, and the air bubbles. In order to verify the ability of the seeding particles to follow the flow, the Stokes Number (Sk) has been calculated as the ratio of the particle response time τ_p to flow characteristic time τ_k:

$$S_k = \frac{\tau_p}{\tau_f} \tag{1}$$

The Stokes Number is equal to 0.016, therefore it satisfies the good flow tracing criterion (Sk<1).
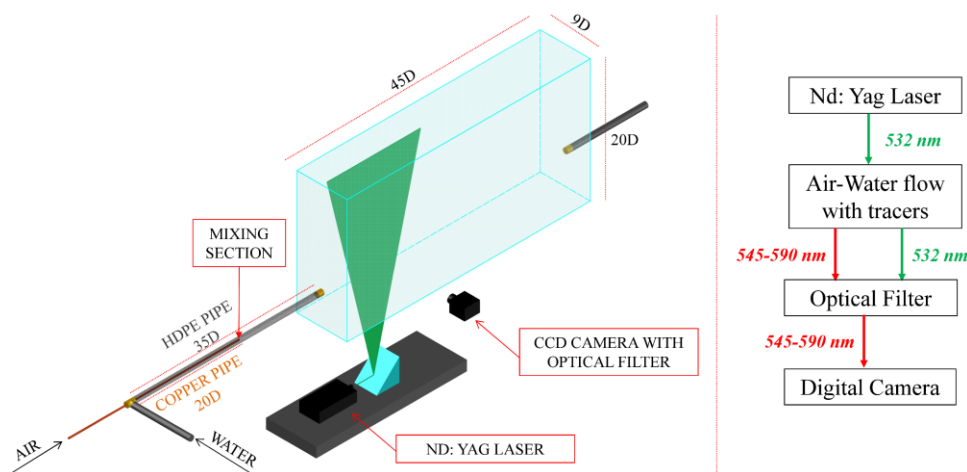
Figure 1. Experimental Setup.

2.2. Discrimination algorithm

In order to carry out a separate analysis of the two phases, it is necessary to divide the information related to the two phases into two distinct images: one containing exclusively tracers (liquid phase) and one containing only the bubbles. The discrimination is based on two main factors: the geometric characteristics of tracers and bubbles and their pixel intensity. As shown in Figure 2, in a PIV-LIF image, the fluorescence emitted by the tracers present the highest level in the grayscale. In addition, the tracers have a size that does not deviate significantly from the average value. The bubbles instead have a significantly variation in terms of size and pixel intensity, with higher values along the perimeter and lower towards the center.
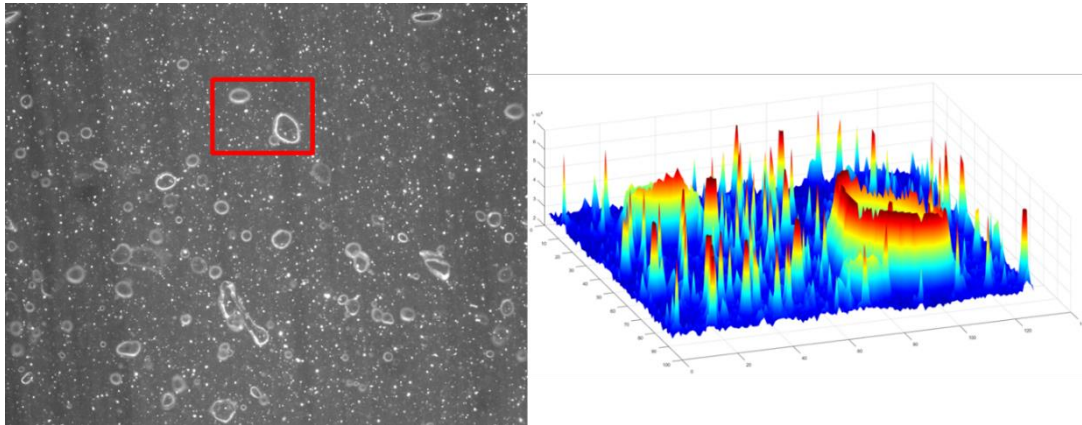
Figure 2. Pixel intensity values of tracers and bubbles.

Based on this information, it has been developed an algorithm able to discriminate the two phases. Figure 3 shows the steps necessary to detect bubbles and tracers and to divide them into distinct images. The first step is the background removal, obtained by subtracting, to each image (Figure 3a), the median image calculated on the entire set of images. The resulting images present only the bubbles and the fluorescence emitted by the tracers (Figure 3b). The next step consists in a binarization of the images (Figure 3c). For this purpose, the IsoData algorithm has been used [8]. As discussed in the previous section, the distinction between the two phases depends on the size and shape of bubbles and tracers. Therefore, a further step is provided for the measure of the area and Euler Characteristic of the objects, bubbles and tracers, in the images. The Euler Characteristic is defined as:

$$Eu = 1 - N_{holes} \tag{2}$$

In the processed images, tracers are objects without holes therefore Eu is equal to 1. Bubbles instead presents a center hole, therefore Eu is equal to 0. In the case of bubble clusters, Eu is less than or equal to -1 depending on the number of bubbles in the cluster, for example for two bubbles Eu is equal to -1, for three bubbles is equal to -2 and so on. Based on the obtained measurements, all the elements with a size smaller than 30 pixels^2 or Eu equal to 1 are considered as tracers while all objects with a size greater than 30 pixels2 or Eu less than 1 are considered as bubbles. The size of 30 pixels^2, equal to 2 time the size of the tracers, takes into account the magnification associated with the scattering. The result is two distinct images of tracers and bubbles, respectively (Figures 3d and 3e).
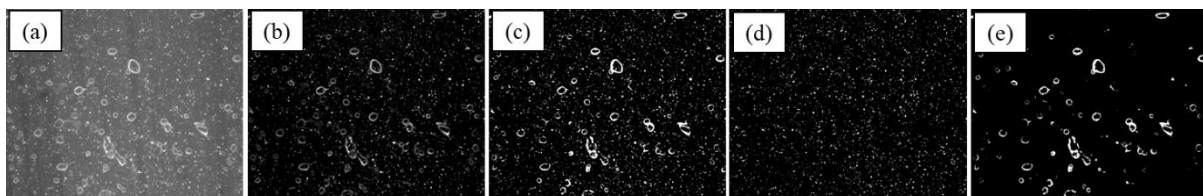
Figure 3. Steps for the detection of the bubbles and tracers.

2.3. Bubbles measurement technique

For the bubbles size analysis, a further selection of the bubbles to be analyzed has been made, identifying those with the best defined contours, with an area-perimeter ratio greater than or equal to 1 (Figure 4b). Since the shape of the bubbles is spherical or ellipsoidal, their measurement has been conducted by means of a direct ellipse fitting algorithm [9]. In order to overcome the bubbles overlapping problem, typically present for bubbles clusters, the watershed technique has been used. This technique treats a grayscale digital image as a topographical surface, with the gray levels of each pixels representing its altitude [10]. Considering a bubbles cluster as a series of hydrographic basins adjacent to each other, the watershed lines allow their division and, consequently, their detection. Following the bubbles detection, the direct ellipse fitting algorithm can be applied, resulting in a bubble characterization expressed in terms of ellipses features (Figure 4c).
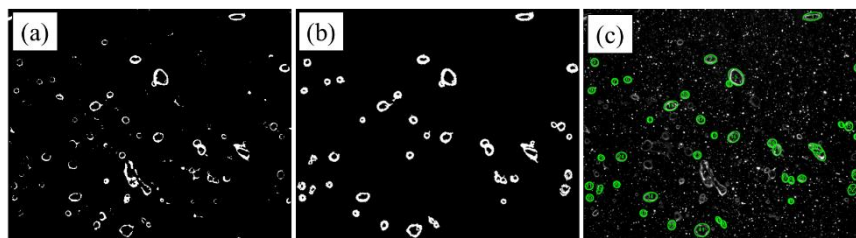
Figure 4. Steps of the bubbles measurement technique.

3. Results and Discussions

PIV analysis has been performed through a correlation based tracking technique called Feature Tracking (FT) implemented in YATS (Yet Another Tracking Software) [11]. The experimental campaign consists of one test set on the single-phase water jet, 2000 couples of frames recorded, and two test sets on the two-phase air-water jet, 4000 couples of frames recorded for each data set. While the water flow rate, equal to 40 l/min, is the same for the three data sets, for the gaseous phase two different values of air flow rate have been defined, equal to 0.1 l/min and 0.2 l/min respectively. The obtained results on the liquid phase of the three data set air-water jet, expressed in terms of velocity and vorticity, are reported in order to describe the flow field of the jet. A comparison between the water jet and the two air-water jet is reported in order to evaluate the incidence of the air bubbles in the air-water jet flow.

Figure 5a shows the mean streamwise velocity, normalized based on the maximum streamwise velocity along the jet axis. It is observed a Gaussian trend with peaks less accentuated as the distance from the outlet section increases, indicating the jet diffusion. In addition, a greater diffusion for the higher air flow rate is observed. The vorticity has been calculated also as:

$$w[1/s] = \frac{dV}{dX} - \frac{dU}{dY} \tag{3}$$

where U and V are respectively the mean horizontal and the mean vertical components of the velocity. Figure 5b shows the vorticity, normalized based on the vorticity peaks. The vorticity is near to 0 along the jet axis with positive and negative peaks respectively at Y=0.25D and Y=-0.25D. An increase of the vorticity is observed in the upper part of the jet for the higher air flow rate.

Figures 6a and 6b show respectively the equivalent diameter of the bubbles and the bubbles numbers. Due to the reduced number of bubbles, the zone below -1D has not been taken into account. The equivalent diameter is in the range 1.2-1.4mm for the lower air flow rate and 1.3-1.7mm for the higher air flow rate. The size increase as increasing the vertical distance from the jet axis. Therefore, larger bubbles rise faster due to the buoyancy force while smaller ones that tend to follow the flow. As shown in Figure 6b, bubbles are in a greater number along the jet axis, decreasing with increasing the vertical distance from the same.
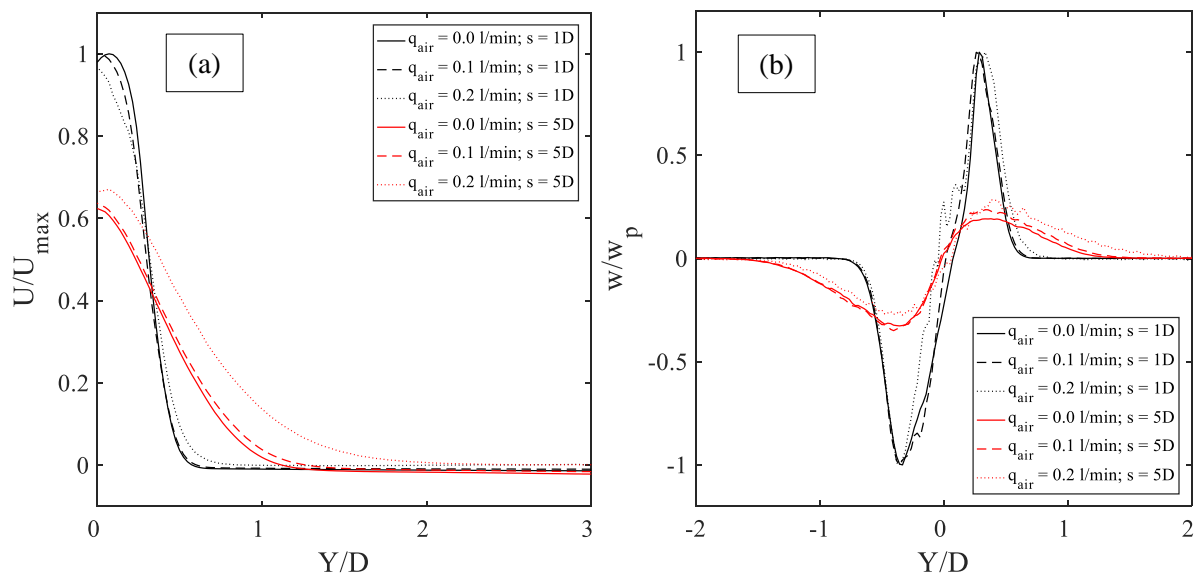
Figure 5. Mean horizontal velocity (a); vorticity (b).
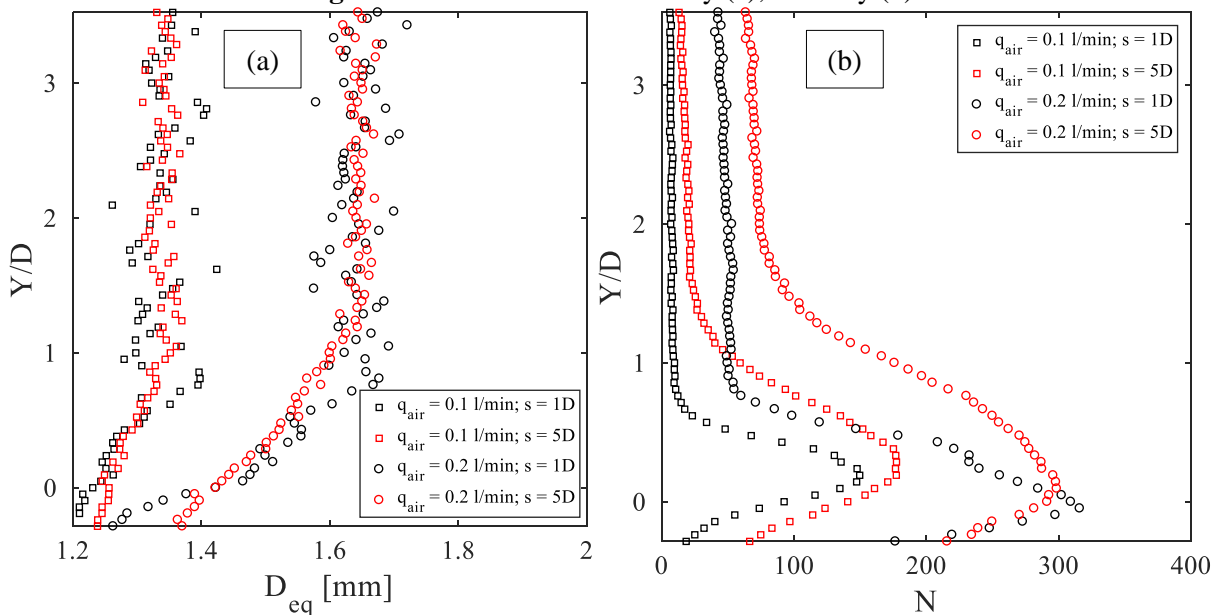
Figure 6. Bubbles equivalent diameter (a); bubbles number (b).

4. Conclusions

An experimental investigation on a two-phase air-water jet is presented. The developed discrimination algorithm allows a proper detection and separation of the two phases with a subsequent accurate analysis of the liquid phase.

Results show that for the higher air flow rate the interaction between the air bubbles and liquid phase has a relevant effect on the flow fields. In particular, a greater diffusion for the higher air flow rate is observed. An analysis on the bubbles size and number is also presented. For the higher air flow rate a greater number of bubbles and a greater size of the same are observed. In the near future, a statistical analysis on the bubbles shape and orientation will be carried out. In addition, bubbles tracking can be an important device for the study of the air bubbles and water interaction.

5. References

[1]   Granata F, de Marinis G, Gargano R and Hager W 2011 Hydraulics of Circular Drop Manholes *J. Irrig. Drain. Eng.* **137** pp 102–111

[2]   Granata F, de Marinis G and Gargano R 2015 Air-water flows in circular drop manholes *Urban Water J.* **12** (6) pp 477–487

[3]   Kodama Y, Kakugawa A, Takahashi T and Kawashima H 2000 Experimental study on microbubbles and their applicability to ships for skin friction reduction *Int. J. Heat Fluid Fl.* **21** (5) pp 582–588

[4]   Merzkirch W, Gui L, Hilgers S, Lindken R, Wagner T 1997 PIV in multiphase flow *Proc. 2nd International Workshop on PIV'97* Fukui, Japan

[5]   Gui L and Merzkirch W 1996 Phase-separation of PIV measurements in two-phase flow by applying a digital mask technique *ERCOFRAC* **30** pp 45–48

[6]   Lindken R and Merzkirch W 2002 A novel PIV technique for measurements in multi-phase flows and its application to two-phase bubbly flows *Exp. Fluids* **33** (6) pp 814–825

[7]   Pedocchi F, Martin J and Garcia M 2008 Inexpensive fluorescent particles for large-scale experiments using particle image velocimetry *Exp. Fluids* **45** (1) pp. 183–186

[8]   Ridler T and Calvard S 1978 Picture thresholding using an iterative selection method *IEEE Trans. Syst. Man Cybern.* **SMC-8** pp 630–632

[9]   Fitzgibbon A, Pilu M and Fisher R 1999 Direct Least Square Fitting of Ellipses *IEEE Trans. on Pattern Anal. Mach. Intell.* **21** (5) pp 476–480

[10]   Najman L and Schmitt M 1994 Watershed of a Continuous Function *Signal Process* **38** (1) pp 99–112

[11]   Miozzi M 2004 Particle Image Velocimetry using Feature Tracking and Delaunay Tessellation *Proc. XII International Symposium on application of laser technique to fluid mechanics* Lisbon, Portugal